Available online at www.sciencedirect.com

SciVerse ScienceDirect

Ceramics International 39 (2013) 5827–5831

CERAMICS INTERNATIONAL

www.elsevier.com/locate/ceramint

The effect of surface area on the photo-catalytic behavior of ZrO_2/carbon clusters composite materials

H. Matsui[a], N. Ohkura[a], S. Karuppuchamy[b,*], M. Yoshihara[a]

[a]*Department of Applied Chemistry, Faculty of Science and Engineering, Kinki University, 3-4-1, Kowakae, Higashiosaka, Osaka 577-8502, Japan*
[b]*Department of Chemistry, Kongu Engineering College. Perundurai, Erode, 638 052 Tamilnadu, India*

Received 17 July 2012; received in revised form 2 January 2013; accepted 2 January 2013

Abstract

Nano-sized ZrO_2/carbon clusters composite materials were successfully prepared by the calcination of a $ZrOCl_2$/starch complex under an argon atmosphere. The obtained composite material was pulverized at 500 °C to obtain powdered materials. The photo-catalytic abilities of the pulverized materials increased with the increase of their surface areas. The visible light induced photo-catalytic activities of the Pt loaded composite materials were also examined.

Keywords: B. Nanocomposites; D. Carbon; Surface area; Photocatalytic activity

---

1. Introduction

Realization of charge-separated electron transfer with photo-responsive function will lead to an achievement of novel photocatalysts. Such charge-separated excitation under light irradiation could be achieved by the use of semiconductors [1–9], however an electron excitation under whole visible light irradiation has not been established yet. We have considered that such an excitation could be achieved by the combination of nano-sized semiconductors and carbon clusters, in which semiconductors are expected to act as a electron excitation site and carbon clusters to act as a visible-light absorption site and an electron transport, resulting in the realization of visible light-responsive electron excitation. We have recently reported the synthesis of such composite materials by the calcination of either metal–organic moiety hybrid copolymers or inorganic metal compound/organic polymer complexes. An efficient visible light-responsive electron transfer between carbon phases and metal compounds was observed for those novel composite materials [10–23]. We have also shown that MnO_2–loaded ZrO_2/carbon clusters composite material could decompose water to H_2 and O_2 under visible light irradiation, however the photo-catalytic activity of the material was rather low [21]. We assume that the lower photo-catalytic activity might be due to a lower surface area of the material, since the surface area of the material was $5\,m^2\,g^{-1}$ which is considerably lower than $50\,m^2\,g^{-1}$ of typical semiconductor TiO_2. In this study, ZrO_2/carbon clusters composite materials I_c's obtained by the calcination of $ZrOCl_2$/starch complex I under an argon atmosphere were pulverized (Scheme 1) and the photo-catalytic activity of the yielded powders were examined.

2. Experimental

2.1. Reagents

Commercially available $ZrOCl_2\cdot8H_2O$, starch, 1,1-diphenyl-2-picrylyhydrazyl (DPPH), methylene blue, citric acid, $AgNO_3$, and hydrogen hexachloroplatinate hexahydrate were used as received.

2.2. Synthesis of complex I

A mixture of 1.08 g (3.34 mmol) of $ZrOCl_2\cdot8H_2O$ and 8.92 g (55 mmol) of starch in 200 mL of distilled water was

---

*Corresponding author. Tel./fax: +91 4294 226555.
E-mail addresses: drskchamy@kongu.ac.in, skchamy@gmail.com (S. Karuppuchamy).

0272-8842/$ - see front matter
http://dx.doi.org/10.1016/j.ceramint.2013.01.003

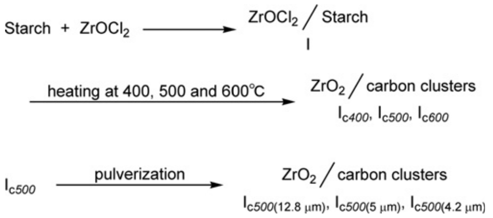

Scheme 1. Synthesis of the materials.

stirred at room temperature for 1 h. Water was evaporated and the residues were dried under a vacuum to obtain I.

2.3. *Calcination of I*

1 g of I in a porcelain crucible was heated with a heating rate of 5 °C/min under an argon atmosphere and kept at 400, 500 and 600 °C for 1 h to obtain calcined materials I_{c400}, I_{c500} and I_{c600}, respectively.

2.4. *Pulverization of I_{c500}*

Three grams of I_{c500} was pulverized with Ishikawa grinding mill AGA to obtain pulverized samples $I_{c500(\mathrm{pul})}$'s, i.e., $I_{c500(12.8\ \mu m)}$, $I_{c500(5\ \mu m)}$ and $I_{c500(4.2\ \mu m)}$, respectively, in which the figures in the parentheses are the average particle diameters of the pulverized materials.

2.5. *Pt-loading on I_{c500} and $I_{c500(4.2\ \mu m)}$*

A mixture of 50 mg of I_{c500} and/or $I_{c500(4.2\ \mu m)}$, 1.2 mL of a degassed 2.11 mmol/L hydrogen hexachloroplatinate aqueous solution and 1.2 mL of methanol was irradiated with light above 460 nm for 1 h. The precipitates were collected, washed with distilled water and dried to obtain Pt-loaded materials I_{c500}Pt and/or $I_{c500(4.2\ \mu m)}$Pt, respectively.

2.6. *Apparatus*

Elemental analysis was performed for C and H using Yanaco MT-6, and for Zr, Ag and Pt by inductively coupled plasma atomic emission spectrometry (ICP-AES) using Shimadzu ICP-7500. X-ray photospectrometry (XPS) spectra were measured using Shimadzu ESCA-850. SEM-EDX spectra were obtained with a Hitachi Hightechnologies S-4800 microscope. Transmission electron microscopy (TEM) observations were done using a Jeol JEM-3010 microscope. Electron spin resonance (ESR) spectra were taken using Jeol JES-TE 200. UV–vis spectra were measured using a Hitachi U-4000 spectrometer. Particle size distribution was analyzed with a Nikkisou Microtrac HRA analyzer. Specific surface area was measured with a Nippon Bell Belsor-Mini adsorber. TCD gas chromatography was taken using Shimadzu GC-8A. Visible light was generated using a Hoya-Shott Megalight 100 halogen lamp.

2.7. *Reduction of methylene blue*

A mixture of 3 mg of I_c's or 1 mg of $I_{c500(\mathrm{pul})}$'s and 10 mL of a 0.03 mmol/L methylene blue–0.12 mmol/L citric acid aqueous solution was stirred in the dark for 48 h. The mixture was irradiated with visible light ($\lambda > 460$ nm) and the concentration of methylene blue was determined by UV–vis spectral analysis.

2.8. *Oxidation–reduction reaction of an aqueous $AgNO_3$ solution with I_{c500} and $I_{c500\ (4.2\ \mu m)}$*

A mixture of 10 mg of the composite material and 1 mL of a 0.05 mol/L $AgNO_3$ aqueous solution was irradiated with visible light ($\lambda > 460$ nm) under an argon atmosphere for 3 h, and then the evolved O_2 gas was analyzed by gas chromatography and the formed Ag was estimated by ICP-AES analysis.

2.9. *Water decomposition*

Ten milligrams of I_{c500} Pt and/or $I_{c500(4.2\ \mu m)}$ in 0.2 mL of degassed water was irradiated with visible light ($\lambda > 460$ nm). Evolved gas was analyzed using gas chromatography.

3. Results and discussion

Complex I was prepared by the procedure described in experimental Section 2.2. SEM-EDX observation of I revealed that Zr atom was uniformly dispersed in the matrix. The calcination of I produced black-colored materials I_c's. Table 1 shows the results of the elemental analysis of complex I and calcined materials I_c's. The increase of the calcination temperature decreases the *H* contents of the materials, suggesting that the carbonization of the materials proceeded. The XPS analyses of I_c's showed a binding energy at 181.7–182.3 eV due to the Zr_{3d} orbital of ZrO_2. The TEM observations of I_c's showed the presence of particles with the diameters of 1–2 nm, possibly ZrO_2, in the matrix. The results indicate that the calcined materials were composed of nano-sized ZrO_2 and carbon clusters. The electronic behaviors of I_c's were examined. Fig. 1 is the ESR spectra of I_c's. A peak at 337 mT ($g = 2.003$) was observed and the highest peak intensity was obtained for I_{c500}. The radical spin quantities (*rsq*) of the calcined materials were determined by a double integrating calculation of the differential absorption line with the use of DPPH and the results are shown in Table 2.

Table 1
Elemental analyses of complex *I* and calcined materials I_c's.

Materials	C (%)	H (%)	Zr (%)	[C]/[Zr]
I	35.9	6.23	2.86	95
I_{c400}	61.8	3.31	6.60	71
I_{c500}	70.4	2.71	9.58	56
I_{c600}	71.7	2.01	9.81	55

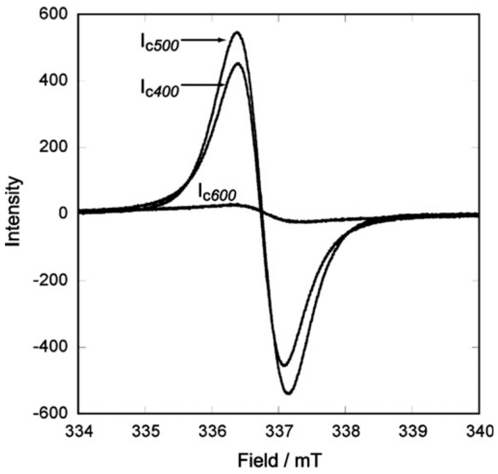

Fig. 1. ESR spectra of calcined materials I_c's.

Table 2
Radical spin quantities (*rsq*) and reduction activities (*ra*) of calcined materials I_c's.

Materials	*rsq* (spin g^{-1})	*ra* (μmol g^{-1} h^{-1})
I_{c400}	1.27×10^{20}	2.26
I_{c500}	2.17×10^{20}	11.8
I_{c600}	6.63×10^{19}	5.01

The highest *rsq* value was observed for I_{c500}. Our understanding is that an electron transfer between ZrO_2 particles and carbon clusters takes place to form a free electron on carbon clusters and the highest electron transfer appeared for I_{c500}. It is noted that the signal intensity increased with the addition of an oxidant (1,4-benzoquinone) but decreased with the addition of a reductant (1,4-hydroquinone), indicating that the signal is due to a radical cation. It is thus deduced that an electron transfer from carbon clusters to ZrO_2 particles takes place to form an oxidation site at carbon clusters and a reduction site at ZrO_2 part.

The photocatalytic activity of the calcined materials was also examined. Fig. 3 is the UV–vis spectra of methylene blue in the presence of I_{c500} under the irradiation of visible light ($\lambda > 460$ nm). The absorption band of methylene blue decreased with the increase of the light irradiation time, indicating that I_{c500} has visible light-responsive reduction ability. The reduction activities (*ra*) of the calcined materials in the reduction reaction of methylene blue were determined by the equation $ra =$ (the amount of methylene blue) (g of the calcined material)$^{-1}$ (h)$^{-1}$, and the results are also shown in Table 2. Here again, the highest *ra* value was observed for I_{c500}, indicating that I_{c500} has the highest photo-reduction ability. I_{c500} was pulverized according to the procedure described in experimental Section 2.4 to obtain pulverized materials $I_{c500(pul)}$'s, i.e., $I_{c500(12.8\ \mu m)}$, $I_{c500(5\ \mu m)}$ and $I_{c500(4.2\ \mu m)}$, respectively. The BET surface area of the pulverized samples was also measured. Table 3 shows the values of the average particle diameters (*apd*) and surface area (*sa*) of the materials. The elemental analysis of the pulverized materials revealed that the C, H and Zr values and [C]/[Zr] ratios of the materials did not vary essentially by the pulverization treatment. The XPS measurements of the pulverized materials showed the presence of a binding energy at 182.0–182.3 eV due to the Zr_{3d} orbital of ZrO_2. The TEM measurements of the pulverized materials also showed the presence of particles with the diameters of 1–2 nm in the matrix (Fig. 2). The results indicated that the pulverization treatment did not change the constituents of the materials. The composite *rsq* and *ra* values of the pulverized materials were determined and the results are also shown in Table 3. The highest *rsq* and *ra* values were observed for $I_{c500(4.2\ \mu m)}$, suggesting that the photo-catalytic ability is affected by the surface area of the materials. The visible light-irradiated oxidation–reduction reaction of an aqueous silver nitrate solution with I_{c500} and $I_{c500(4.2\ \mu m)}$ was performed and the results are shown in Table 4. The amounts of Ag and O_2 formed for $I_{c500(4.2\ \mu m)}$ was found to be higher than those for I_{c500}, indicating that the increase of the surface area of the material and thereby exhibits increased photo-catalytic activity. Here, if a four electron oxidation-reduction reaction takes place, then a [Ag]/[O_2] ratio is given to be 4. The observed [Ag]/[O_2] ratios were to be close to 4, suggesting an occurrence of a rather smooth electron excitation.

It is known that the loading of Pt on semiconductors increases the reduction ability. The surfaces of I_{c500} and $I_{c500(4.2\ \mu m)}$ were thus modified with Pt particles by reacting with a hydrogen hexachloroplatinate aqueous methanol solution under visible-light irradiation according to the procedure described in experimental Section 2.5 to obtain Pt-loaded materials I_{c500}Pt and $I_{c500(4.2\ \mu m)}$Pt, respectively. ICP-AES analysis of the Pt-loaded materials showed the contents of Pt of 0.12 wt% for I_{c500}Pt and 0.51 wt% for $I_{c500(4.2\ \mu m)}$Pt, respectively. TEM observations of the materials reveal the presence of highly dispersed Pt particles with the diameters of ca. 5–10 nm on the surfaces of the materials. XPS spectra of the materials showed the presence of a peak of $4f_{7/2}$ orbital of Pt at 70.8–71.1 eV. Water decomposition experiments with I_{c500}Pt and $I_{c500(4.2\ \mu m)}$Pt under the irradiation of visible light ($\lambda > 460$ nm) were carried out to obtain H_2 of 8 and 24 nmol, respectively, suggesting that the photo-catalytic ability was enhanced by the increase of surface area. However, it must be indicated that there was no O_2 evolution detected. H_2 evolution suggested that reduction energy is sufficient to decompose water at the reduction site, i.e. Pt, and the oxidation of water at the oxidation site, i.e. the carbon clusters. A possible assumption for non-generation of O_2 is that an activated species formed at the oxidation site may be trapped possibly by the carbon clusters to decrease the oxidation ability of the oxidation site without O_2 formation.

4. Conclusions

Nano-sized ZrO_2/carbon clusters composite materials were obtained by the calcination of a $ZrOCl_2$/starch complex under

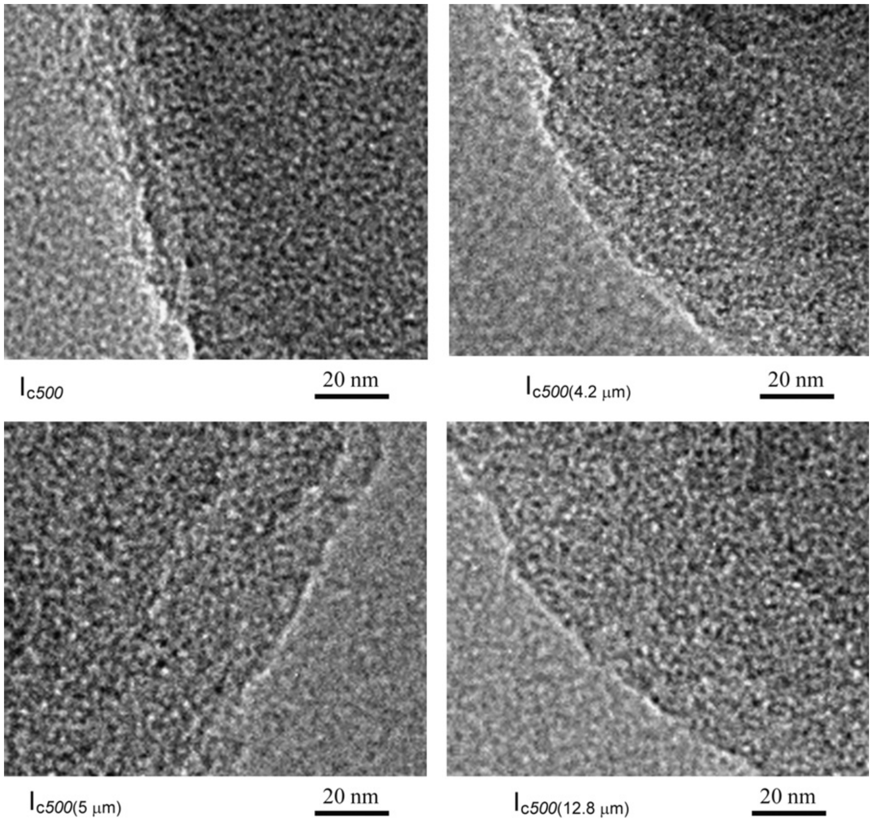

Fig. 2. TEM images of Calcined materials.

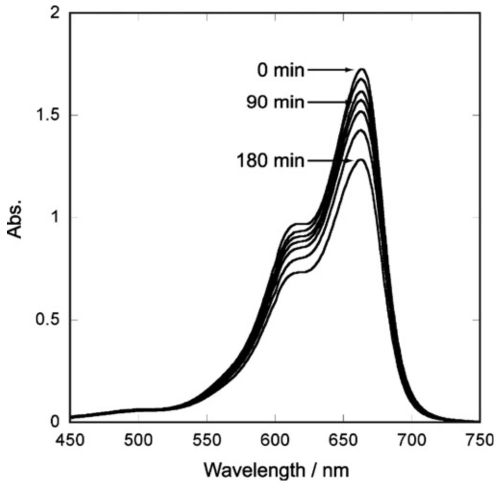

Fig. 3. UV–vis spectra of methylene blue in the presence of I_{c500} under the irradiation of light ($\lambda > 460$ nm).

an argon atmosphere. In order to investigate the effect of surface area on the photo-catalytic activity of the composite materials, materials were pulverized. The pulverized composite materials show high surface area. The present investigation clearly demonstrates that the catalytic activity of the pulverized materials increased with the increase of the surface area. The findings will contribute to develop a novel and efficient photocatalysts.

Table 3
Average particle diameters (*apd*), surface areas (*sa*), radical spin quantities (*rsq*) and reduction activities (*ra*) of I_{c500} and $I_{c500(\text{pul})}$'s.

Materials	*apd* (μm)	*sa* ($m^2\ g^{-1}$)	*rsq* ($\text{spin}\ g^{-1}$)	*ra* ($\mu\text{mol}\ g^{-1}\ h^{-1}$)
I_{c500}	28.1	5.0	2.17×10^{20}	11.8
$I_{c500(12.8\ \mu m)}$	12.8	31.7	1.71×10^{20}	10.1
$I_{c500(5\ \mu m)}$	5.0	63.9	2.16×10^{20}	18.0
$I_{c500(4.2\ \mu m)}$	4.2	155.0	2.56×10^{20}	19.4

Table 4
Amounts of Ag and O_2 formed in the decomposition reaction of an aqueous $AgNO_3$ solution in the presence of calcined materials under the irradiation of light above 460 nm.

Materials	$\mu\text{mol}\ g^{-1}\ h^{-1}$		Ratios
	Ag	O_2	[Ag]/[O_2]
I_{c500}	222	58	3.8
$I_{c500(4.2\ \mu m)}$	275	71	3.9

Acknowledgment

This work was supported by a Grant-in-aid for scientific research (B) 21310076 from the Ministry of Education, Science, Sports and Culture, Japan.

References

[1] Z. Zou, J. Ye, K. Sayama, H. Arakawa, Direct splitting of water under visible light irradiation with an oxide semiconductor photocatalyst, Nature 414 (2001) 625–627.

[2] A. Fujishima, K. Honda, Electrochemical photolysis of water at a semiconductor electrode, Nature 238 (1972) 37–38.

[3] K. Sayama, K. Musaka, R. Abe, Y. Abe, H. Arakawa, Stoichiometric water splitting into H_2 and O_2 using a mixture of two different photocatalysts and an IO_3^-/I^- shuttle redox mediator under visible light irradiation, Chemical Communications (2001) 2416–2417.

[4] N. Okada, S. Karuppuchamy, M. Kurihara, An efficient dye-sensitized photoelectrochemical solar cell made from $CaCO_3$- coated TiO_2 nanoporous film, Chemistry Letters (2005) 16–17.

[5] H. Kato, M. Hori, R. Konta, Y. Shimodaira, A. Kudo, Construction of z-scheme type heterogeneous photocatalysis systems for water splitting into H_2 and O_2 under visible light irradiation, Chemistry Letters 33 (2004) 1348–1349.

[6] R. Konta, T. Ishii, H. Kato, A. Kudo, Photocatalytic activities of noble metal ion doped $SrTiO_3$ under visible light irradiation, Journal of Physical Chemistry B 108 (2004) 8992–8995.

[7] X. Zong, Photocatalytic H_2 evolution on MoS_2/CdS catalysts under visible light irradiation, Journal of Physical Chemistry C 114 (2010) 1963–1968.

[8] J.S. Zhang, Synthesis of a carbon nitride structure for visible-light catalysis by copolymerization, Angewandte Chemie International Edition 49 (2010) 441–444.

[9] X.C. Wang, A metal-free polymeric photocatalyst for hydrogen production from water under visible light, Nature Materials 8 (2009) 76–82.

[10] T. Furukawa, H. Matsui, H. Hasegawa, S. Karuppuchamy, M. Yoshihara, The electronic behaviors of calcined materials from a (S-nickel-S-phenylene-O)–strontium–(O-phenylene-S-selenium-S) hybrid copolymer, Solid State Communications 142 (2007) 99.

[11] T. Kawahara, H. Miyazaki, S. Karuppuchamy, H. Matsui, M. Ito, M. Yoshihara, Electronic nature of vanadium nitride–carbon cluster composite materials obtained by the calcination of oxovanadylphthalocyanine, Vacuum 81 (2007) 680.

[12] T. Kawahara, T. Kuroda, H. Matsui, M. Mishima, S. Karuppuchamy, Y. Seguchi, M. Yoshihara, Electronic properties of calcined materials from a scandium-O-phenylene-O-yttrium-O-phenylene hybrid copolymer, Journal of Materials Science 42 (2007) 3708.

[13] H. Matsui, S. Karuppuchamy, J. Yamaguchi, M. Yoshihara, Electronic behavior of calcined materials from SnO_2 hydrosol/starch composite materials, Journal of Photochemistry and Photobiology A: Chemistry 189 (2007) 280.

[14] H. Miyazaki, H. Matsui, T. Nagano, S. Karuppuchamy, S. Ito, M. Yoshihara, Synthesis and electronic behaviors of TiO_2/carbon clusters/Cr_2O_3 composite materials, Applied Surface Science 254 (2008) 7365.

[15] H. Miyazaki, H. Matsui, Y. Kita, S. Karuppuchamy, S. Ito, M. Yoshihara, Electronic behavior of visible light sensitive ZrO_2/Cr_2O_3/carbon clusters composite materials, Current Applied Physics 9 (2009) 155.

[16] H. Matsui, T. Kuroda, T. Kawahara, S. Karuppuchamy, R. Kudo, M. Yoshihara, Electronic behavior of visible light sensitive ZrO_2/Cr_2O_3/carbon clusters composite materials, Current Applied Physics 9 (2009) 263.

[17] H. Matsui, S. Yamamoto, T. Sasai, S. Karuppuchamy, M. Yoshihara, Electronic behavior of WO_2/carbon clusters composite materials, Electrochemistry 75 (2007) 345.

[18] H. Matsui, T. Okajima, S. Karuppuchamy, M. Yoshihara, The electronic behavior of V_2O_3/TiO_2/carbon clusters composite materials obtained by the calcination of a $V(acac)_3$/$TiO(acac)_2$/polyacrylic acid complex, Journal of Alloys and Compounds 468 (2009) L27.

[19] H. Matsui, N. Bando, S. Karuppuchamy, J-M. Jeong, M. Yoshihara, Synthesis and characterization of ZrO_2/MnO_2/carbon clusters composite materials, Superlattices and Microstructures 50 (2011) 427.

[20] S. Karuppuchamy, H. Matsui, K. Kira, M.A. Hassan, M. Yoshihara, Visible light induced photocatalytic activity of Nb_2O_5/carbon cluster/Cr_2O_3 composite materials, Ceramics International 38 (2012) 1515.

[21] H. Matsui, N. Bandou, S. Karuppuchamy, M.A. Hassan, M. Yoshihara, Efficient photocatalytic activity of MnO_2-loaded ZrO_2/carbon clusters nanocomposite materials under visible light irradiation, Ceramics International 38 (2012) 1605.

[22] H. Matsui, M. Nishii, S. Karuppuchamy, J.-M. Jeong, M.A. Hassan, M. Yoshihara, Visible light induced electron transfer behavior of a novel CeO_2-loaded HfO_2/Carbon cluster composite materials, Journal of Alloys and Compounds 513 (2012) 184.

[23] L. Zhao, X. Chen, X. Wang, Y. Zhang, W. Wei, Y. Sun, M. Antonietti, M.-M. Titirici, One-step solvothermal synthesis of a carbon@TiO_2 dyad structure effectively promoting visible-light photocatalysis, Advanced Materials 22 (2010) 3317.